PORTLAND
PRESS

Research Article

Thousand and one kinase 1 protects MCAO-induced cerebral ischemic stroke in rats by decreasing apoptosis and pro-inflammatory factors

Jiahui Li[1], Zhijie Liu[1], Liling Wang[1], Haiyan Xu[1] and Yulin Wang[2]

[1]Department of Neonatal Intensive Care Unit, Shandong Provincial Qianfoshan Hospital, Shandong University, Jinan 250014, Shandong, China; [2]Department of Pediatric Cardiology, Shandong Provincial Hospital Affiliated to Shandong University, Jinan 250014, Shandong, China

Correspondence: Yulin Wang (wangyulin2116@163.com)

Background: Birth hypoxia causes neonatal mortality and morbidity. Hypoxia/ischemia can facilitate brain damage, causing various kinds of diseases, such as ischemic stroke. It is necessary to understand the potential underlying mechanisms of ischemic stroke. Previous studies revealed the involvement of thousand and one kinase 1 (TAOK1) in many cellular processes. **Methods:** Herein, middle cerebral artery (MCA) occlusion (MCAO) was performed in rats to establish ischemic stroke in the animal model, and cortical neural stem cells from rats were treated with oxygen-glucose deprivation (OGD) to induce ischemic stroke cell model. The animal model of ischemic stroke was validated by Bederson and Zea-Longa neurological deficit scores and rotarod test. TAOK1 expression was examined by quantitative real-time PCR (qRT-PCR), Western blot, and immunofluorescent staining both *in vivo* and *in vitro*. **Result:** Compared with sham animals, the MCAO rats showed a significant increase in the neurological scores, and obvious motor behavioral deficits. Meanwhile, there was increased apoptosis and inflammatory response in the model group. TAOK1 overexpression reversed the OGD-induced cell injury, while TAOK1 knockdown exhibited the opposing effects. On the mechanism, the OGD-induced suppression of PI3K/AKT, and activation of mitogen-activated protein kinase (MAPK) signaling pathways were abolished by TAOK1 overexpression, and aggravated by TAOK1 knockdown *in vitro*. Moreover, we proved that the inhibitory effect of TAOK1 on OGD-induced apoptosis was dependent on the intracellular kinase activity. **Conclusion:** TAOK1 protected MCAO-induced cerebral ischemic stroke by decreasing the pro-inflammatory factors and apoptosis via PI3K/AKT and MAPK signaling pathways.

Introduction

Hypoxic–ischemic encephalopathy (HIE) is a major cause of neonatal death, resulting in long-term neurological dysfunction. It is estimated that 23% of all newborns die due to HIE worldwide, i.e. a total of 1 million per year [1]. 25% of the surviving children suffer from severe long-term neurological dysfunction. Currently, HIE is one of the top ten diseases with the greatest lifelong burden all over the world [2]. Research efforts over decades have indicated that hypoxia/ischemia could easily cause ischemic stroke [3–6]. The large quantity of statistical data also indicated that neonatal stroke occupies approximately 1/4000 live babies, causing lifelong nerve damage, such as cerebral palsy [7]. Despite the enormous efforts put in understanding the potential mechanisms of ischemic stroke, it largely remains unknown. Tissue plasminogen activator (tPA) is the only drug approved by the Food and Drug Administration (FDA) for ischemic stroke to date, and has limited effects due to its remarkably short therapeutic time window [8–10]. Therefore, it

1

is necessary to investigate the mechanistic basis of ischemic stroke, and explore several new therapeutic targets.

Thousand and one kinases (TAOKs) is an important subfamily of germinal-center kinase-like class of sterile 20 (Ste20)-like kinases, consisting of TAOK1, TAOK2, and TAOK3 [11]. Previous studies have revealed that TAOKs were involved in the regulation of mitogen-activated protein kinase (MAPK) signaling pathway, and the TAOKs subfamily, except TAOK3, could activate c-Jun N-terminal kinase (JNK) during DNA damage and environmental stress conditions [12–14]. TAOK1 also acts as a critical regulator for microtubule dynamics and mitotic processes by interacting with a spindle checkpoint component [15,16]. Moreover, TAOK1 assists in cell morphological alterations of apoptosis by regulating JNK and MAPK signaling pathway [17]. Recently, TAOK1 was regulated by microRNAs (miRNAs) in various cellular processes [18,19]. However, whether TAOK1 plays a role in the pathogenesis of ischemic stroke still remains unclear.

In the present study, we aimed to investigate the roles of TAOK1 in ischemic stroke. We initially examined the expression of TAOK1 in middle cerebral artery (MCA) occlusion (MCAO) rat model, which is the most frequently used animal model of ischemic stroke. In the subependymal ventricular zone (SVZ) of MCAO rats, TAOK1 expression was significantly down-regulated, however, the IL-1β, IL-6, and IL-8 expressions were up-regulated than those of sham rats. We then performed TAOK1 gain- and loss-of functions in the oxygen-glucose deprivation (OGD) induced *in vitro* neural stem cell model of ischemic stroke. The results indicated that overexpression of TAOK1 ameliorated the OGD-induced cell injury, and knockdown of TAOK1 exacerbated OGD-induced cell injury. The underlying mechanism revealed the involvement of PI3K/AKT and MAPK signaling pathway in the protective effects of TAOK1 in ischemic stroke. These results suggested the protective role of TAOK1 against MCAO-induced cerebral ischemic stroke by decreasing the pro-inflammatory factors via PI3K/AKT and MAPK signaling pathways.

Materials and methods
Animals and establishment of ischemic stroke animal model

A total of 36 male SD rats (300–320 g) were obtained from Beijing Vital River Laboratory Animal Technology Co., Ltd (Beijing, China), and were used in the present study according to the procedures approved by the Institutional Animal Care and Use Committee (IACUC) of Shandong University. All animal experiments were performed at Shandong University and guided by IACUC. The rats were maintained at 22–25°C, 50% humidity, and 12-h light/dark cycle. The rats were randomly divided into two groups: sham group and MCAO group. For establishing the MCAO animal model, the rats were initially anesthetized with 4% pentobarbital sodium. After that, the external carotid artery (ECA) of the rat was tied, and the monofilament nylon sutures (4-0) were inserted from the common carotid artery (CCA) to the internal carotid artery (ICA) via ECA. The monofilament nylon sutures were then used to block the left MCA at its origin (18 mm). After ischemia for 2 h, the plug was removed for reperfusion. For sham animals ($n=18$), all the protocols were performed similar to the establishment of MCAO model, except the occlusion of MCA.

Evaluation of neurological deficits

The neurological deficits of MCAO ($n=18$) and sham rats ($n=18$) were assessed by using the Bederson and Zea-Longa neurological deficit scores. In brief, score 0 indicates no visible neurological deficits; score 1 indicates mild neurological disorders, such as dysfunction in stretching the anterior limb; score 2 was given to those animals that circle unidirectionally when the animal is pulled by the tail; score 3 was given to those that show rolling movement; score 4 was given to those animals with reduction in consciousness; score 5 indicates death.

2,3,5-triphenyltetrazolium chloride staining

The infarct volume of brain of MCAO rats was evaluated using 2,3,5-triphenyltetrazolium chloride (TTC) staining. Briefly, the brains of MCAO and sham rats were dissected and cut into 2-mm slices (coronal). The brain slices were incubated with 2% TTC solution for 20 min at 37°C, followed by draining off excessive TTC solution, and fixing the brain slices with 4% formalin. The volume of infarct area was quantified using the ImageJ analysis system.

Rotarod test

The rotarod test was carried out to assess the motor function of sham and MCAO animals. The rats were placed on an accelerating rotating rod (from 0 to 40 rpm over 5 min) and their speed and distance to fall off the rod were recorded. Before the experiment, the rats were trained for 3 days consecutively (three times/day).

RNA extraction and quantitative real-time PCR assay

Total RNAs of SVZ brain area and neural stem cells were extracted by TRIzol reagent (#9109, Takara, Japan), and 2 µg of total RNAs were used as template to reverse transcribe into cDNA using Bestar qPCR RT Kit following the instructions of manufacturers. Real-time quantitative PCR amplification was carried out on ABI7000 system with the following reaction system: Bestar® Sybr Green qPCR Master Mix 10 µl, forward primer (10 µM) 0.5 µl, reverse primer (10 µM) 0.5 µl, cDNA 1 µl, ddH$_2$O 8 µl. The sequence of primers used was as follows: GAPDH F: 5′-CCTCGTCTCATAGACAAGATGGT-3′, R: 5′-GGGTAGAGTCATACTGGAACATG-3′; TAOK1 F: 5′-AAG AGC ATC AGC TCC ACA GT-3′, R: 5′-GCC GAT GTT CGT CCA TTT CT-3′; and the mRNA expression of TAOK1 was normalized to GAPDH.

Western blot assay

Proteins of SVZ area and neural stem cells were prepared using RIPA buffer followed by high-speed centrifugation (12000 rpm, 20 min) at 4°C. After collecting the supernatants, the protein concentration was determined by BCA kit, and 40 µg of total proteins were isolated with 10% SDS/PAGE. The targeted proteins were transferred on to nitrocellulose membranes (Millipore, Billerica, MA, U.S.A.) and then incubated with 5% low-fat dried milk for 2 h to block the non-specific binding sites. The primary antibodies were used to incubate with membranes at 4°C overnight. After washing with PBS twice, the membranes were incubated with horseradish peroxidase–conjugated secondary antibodies for 2 h, and then the signals were detected by enhanced chemiluminescent reagents. The antibodies in the present study included TAOK1 (Rabbit, 1:1000, ab197891, Abcam), GAPDH (1:3000, sc420485, Santa Cruz), AKT (Rabbit, 1:1000, ab106693, Abcam), p-AKT (Rabbit, 1:1000, ab38449, Abcam), Bax (Rabbit, 1:1200, ab263897, Abcam), Bcl-2 (Rabbit, 1:1200, ab196495, Abcam), Cleaved-caspase-3 (Rabbit, 1:1000, ab2302, Abcam), CyclinD1 (goat, 1:1500, ab194972, Abcam), extracellular signal-regulated kinase (ERK) (Rabbit, 1:1000, ab137619, Abcam), p-ERK (Rabbit, 1:1000, ab79483, Abcam), P-21 (Mouse, 1:1000, ab168220, Abcam), PI3K (Rabbit, 1:1200, ab70912, Abcam), P38 (Rabbit, 1:1000, ab27986, Abcam), p-P38 (Rabbit, 1:1000, ab47363, Abcam).

Immunofluorescent staining

For TAOK1 immunofluorescent staining of brain slice, after fixing the brain slice in 4% formalin overnight, and dehydrated in 10, 20 and 30% sucrose solutions for 3 days, the brain area containing SVZ was cut into 35-µm sections. For TAOK1 immunofluorescent staining of neural stem cells, the neural stem cells were collected and washed twice with PBS, and then fixed in 4% formalin overnight. After blocking with 10% donkey serum for 2 h, the brain sections and fixed neural stem cells were initially incubated with primary antibodies against TAOK1 (Rabbit, 1:500, ab150519, Abcam) for overnight at 4°C. After washing with PBS for three times (10 min/time), the brain slices and neural stem cells were stained with anti-rabbit secondary antibody-546 for 2 h, and incubated in DAPI for 10 min. The signals were detected with a laser confocal fluorescence microscopy (Leica, Germany). The neural stem cells were additionally stained with Nestin (Mouse, ab6142, 1:1000, Abcam), GFAP (Rabbit, ab7260, 1:1000, Abcam), and Tuj1 (Rabbit, ab18207, 1:1000, Abcam) as described above.

TUNEL assay

The brain sections and neural stem cells used in the immunofluorescent staining were utilized for the detection of damaged cells in TUNEL assay using a Fluorescein *In Situ* Cell Death Detection Kit (Roche Diagnostics GmbH, Mannheim, Germany). After washing with PBS, the sections and cells were incubated for 10 min with pre-cold ethanol-acetic solution (3:1), followed by incubation with 5% Triton-X 100 (Sigma). Subsequently, the sections and cells were incubated 90 min with TdT-enzyme buffer supplemented with fluorescein-dUTP, followed by Hoechst 33258 (Invitrogen, Germany). The signals were detected by a laser confocal fluorescence microscopy (Leica, Germany).

Enzyme-linked immunosorbent assay

The production of IL-1β, IL-6, and IL-8 in the SVZ brain area and treated neural stem cells were assessed by enzyme-linked immunosorbent assay (ELISA). Then the SVZ and neural stem samples were used in Western blot assay for the detection of IL-1β, IL-6, and IL-8 by ELISA. In brief, after lysis in RIPA buffer, the production of IL-1β (Elabscience, E-EL-R0012), IL-6 (Elabscience, E-EL-R0015), and IL-8 (Shanghai enzyme linked, ml037351) in the supernatants of SVZ and cells were evaluated by corresponding ELISA kit according to the manufacturer's instructions.

Primary cortical neuron stem culture and OGD

The primary neural stem cells were obtained from the cerebral cortex of embryo at 18 days gestation rats as described previously [20]. In brief, the cerebral cortices were digested with 0.25% trypsin, and then the cell suspension was seeded into six-well plates pre-coated with poly-L-lysine. The cells were maintained in DMEM containing 10% fetal bovine serum and cytosine-D-arabinofuranoside (10 μM) under 95% air, 5% CO_2, and humidified conditions. For OGD treatment, the cortical neurons were previously cultured in DMEM under normal conditions for 12 h, followed by incubation with glucose-free Earle's balanced salt solution supplemented with 0.5 mmol/l sodium dithionite (de-oxygenated reagent) under hypoxic conditions (95% N_2 and 5% CO_2) for 2 h. The culture medium was changed every 2 days. After 7 days of cell culture, the cells were used for subsequent experiments.

Cell counting kit-8 assay

The effects of TAOK1 on cell proliferation were assessed by using a cell counting kit-8 (CCK-8, Dojindo Laboratories, Japan). In brief, the treated neural stem cells were collected and plated into 96-well plates at a concentration of 2×10^4 cells/well. Then cell viability was detected at 24, 48, and 72 h after seeding using a microplate reader at 450 nm.

EdU staining

Cell-light EdU Apollo 546 *in vitro* kit (RiboBio) was utilized to further evaluate cell proliferation of treated neural stem cells following the manufacturer's instructions. Briefly, the treated neural stem cells were collected and plated into six-well plates with 1 ml medium, making the final concentration of 1×10^5 cells/well. After culturing overnight, the medium was replaced with fresh medium containing EdU (100 μM) and incubated for 2 h. Subsequently, the cells were fixed in acetone for 20 min, followed by incubation with Apollo reaction buffer supplemented with FITC-fluorescein for 1 h. The signals were then examined using a laser confocal fluorescence microscope (Leica, Germany).

Cell cycle analysis

The treated neural stem cells were cultured at 37°C in six-well plates until the cells reached 80% confluence, and then were collected and fixed with 70% pre-cold ethanol for 2 h. After washing twice with PBS, the treated neural stem cells were re-suspended in 0.5 ml PBS supplemented with propidium iodide (PI, 60 μg/ml), and incubated at room temperature for 30 min. The cell cycle was analyzed with a FACS Calibur Flow Cytometer (BD Biosciences, U.S.A.).

Flow cytometry apoptosis assay

The treated neural stem cells were harvested and re-suspended in staining buffer containing 60 μg/ml PI and Annexin V, and maintained at room temperature for 15 min in the dark. Subsequently, the ACS Calibur Flow Cytometer (BD Biosciences, U.S.A.) was used to analyze the cell apoptosis.

Statistical analysis

All data were presented as means ± SEM from three repeated experiments. Statistical analysis was performed using GraphPad (Ver. Prism 7, GraphPad Prism Software, La Jolla, CA, U.S.A.) with one-way analysis of variance or Student's *t* test. Differences between the means were considered significant if *P*-values were less than 0.05.

Results
Verification of MCAO rat model

To investigate the role of TAOK1 in brain ischemic stroke, an experimental model of brain ischemic stroke MCAO was established. The MCAO rat model was verified by examining the neurological deficits with Bederson/Longa scores, and rotarod test at 14 days after MCAO. Compared with sham animals, MCAO rats showed a significant increase in the neurological scores (***P<0.001 *vs* sham group, Figure 1A,B). The results from TTC staining showed an extensive infarction area in a large proportion of ipsilateral hemisphere of MCAO rats (Figure 1C). In addition, compared with sham group, the MCAO rats exhibited obvious motor behavioral deficits in the average speed, nextime, distance, and revolving speed of rotarod test (***P<0.001 *vs* sham group, Figure 1D–G). These results suggested that the construction of a rat model of brain ischemic stroke was successfully established.
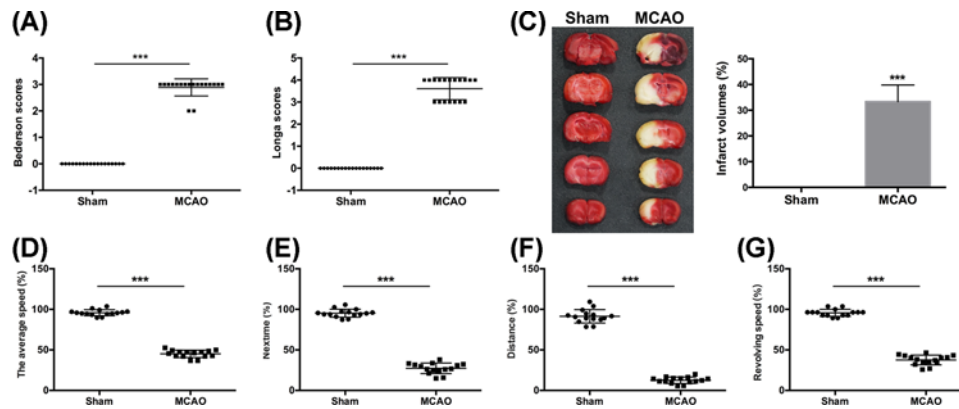
Figure 1. MCAO rats exhibited neurological and functional deficits

(**A**,**B**) Neurological deficient MCAO rats were evaluated by Bederson and Longa scores (***$P<0.001$ *vs* Sham). (**C**) The infarct volume of sham and MCAO rats was assessed. (**D**–**G**) Rotarod test was performed to analyze the motor function of MCAO rats (***$P<0.001$ *vs* Sham).

TAOK1 expression was decreased, apoptosis and inflammation were enhanced in the SVZ of MCAO rats

We then investigated the expression of TAOK1 in SVZ by quantitative real-time PCR (qRT-PCR), Western blot, and immunohistochemical analysis. Compared with sham group, the relative mRNA expression of TAOK1 was significantly reduced in the SVZ of MCAO rats (**$P<0.01$, Figure 2A). Western blotting results demonstrated a significant down-regulation of TAOK1 protein expression in the SVZ of MCAO rats compared with sham animals (Figure 2B). In addition, we identified the distribution of the neural stem cells in the brain slices by immunofluorescent staining. We found that TAOK1 and Nestin were highly expressed in the brain of MCAO rats (Supplementary Figure S1A), meanwhile, the results revealed that TAOK1 and Nestin were widely distributed in in the SVZ of brain (Supplementary Figure S1). Immunohistochemical analysis also showed that the staining intensity of TAOK1 in the SVZ brain slice of MCAO rats was significantly attenuated compared with sham group (Figure 2C). Moreover, TUNEL assay was carried out to detect the apoptosis of neural stem cells of SVZ brain slice in sham and MCAO rats. The results showed a significant increase in the apoptotic rate in the SVZ brain slice of MCAO rats when compared with sham group (Figure 2D). In addition, ELISA was performed to evaluate the production of IL-1β, IL-6, and IL-8, and the results showed that their expression levels were remarkably increased in the blood samples collected from MCAO rats when compared with blood samples collected from sham rats (**$P<0.01$, Figure 2E).

TAOK1 expression was significantly decreased post-OGD in neural stem cells

An *in vitro* model of ischemic stroke was established using cortical neural stem cells collected from fetal rats at 18 days of gestation. The purity of the neural stem cells was verified by Nestin, GFAP, Tuj1, and DAPI staining. The cultures showed an obvious Nestin positive signal and GFAP/Tuj1 negative signal, suggesting that the majority of the cells in the cultures were neural stem cells (Figure 3A). We then detected the expression of TAOK1 in OGD-treated neural stem cells, and the results suggested that TAOK1 mRNA and protein expression in OGD-treated neural stem cells were significantly decreased when compared with normal neural stem cells (***$P<0.001$ *vs* normal group, Figure 3B,C). Immunofluorescent staining of TAOK1 in OGD-treated cells showed remarkably attenuated signals compared with normal cells (Figure 3D). To investigate the effects of TAOK1 on OGD-induced in *in vitro* ischemic stroke cell model, short hairpin RNA (shRNA) or recombinant plasmid of TAOK1 was utilized to knockdown or overexpress TAOK1 expression in OGD-treated neural stem cells. The knockdown and overexpression efficiency of TAOK1 in neural stem cells under OGD was determined by Western blot, qRT-PCR, and immunofluorescent staining. The results showed that the TAOK1 expression was significantly down-regulated in OGD+shRNA group, whereas remarkably up-regulated in OGD+TAOK1 group, compared with OGD+NC group (###$P<0.001$ *vs* OGD+NC group, Figure 3B–D).
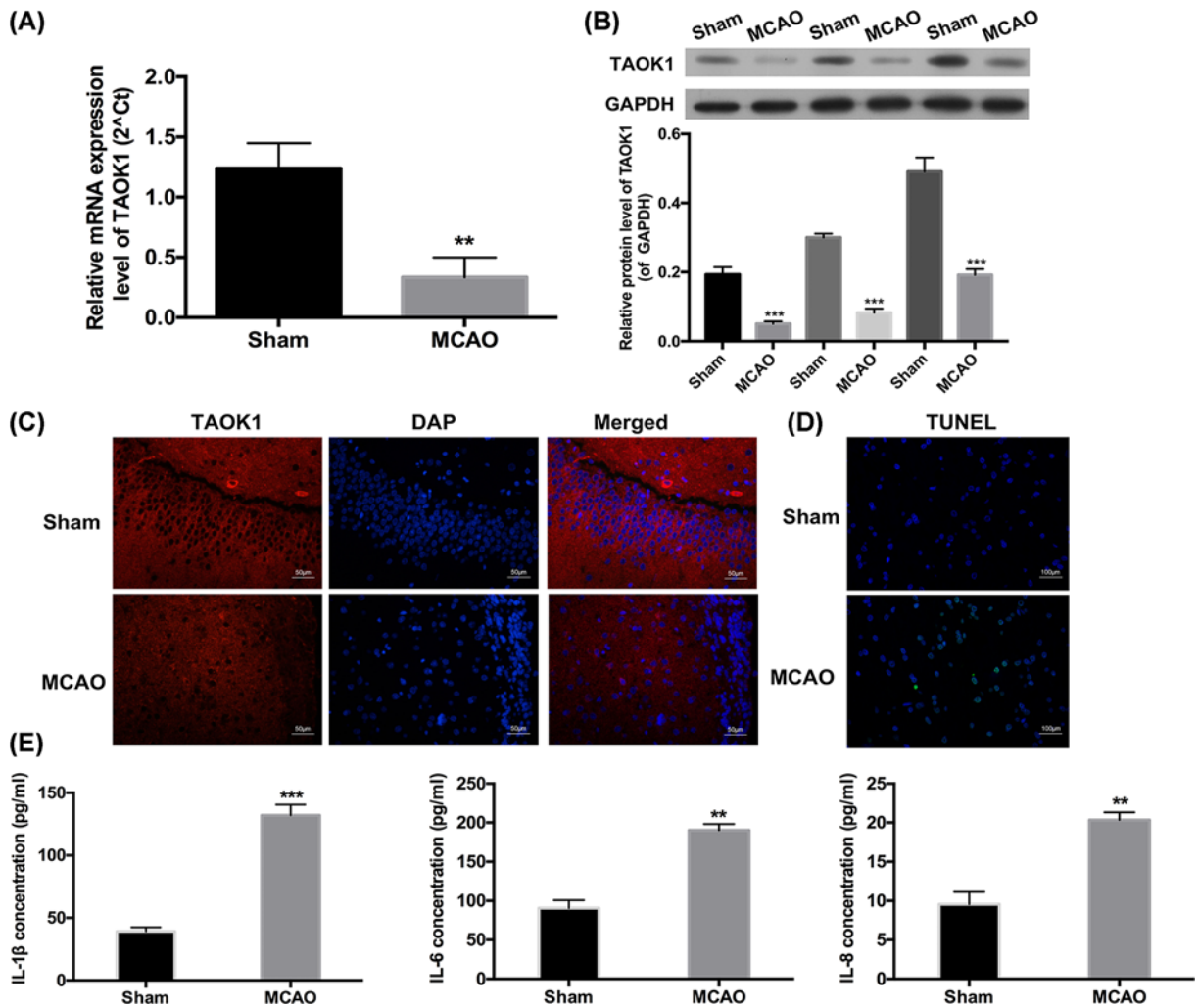
Figure 2. The changes in TAOK1 expression, apoptosis and inflammation in the SVZ of MCAO rats

(**A,B**) Relative mRNA and protein expression of TAOK1 in the SVZ of sham and MCAO rats were assessed by qRT-PCR and Western blotting assays, respectively (**$P<0.01$ *vs* Sham). (**C**) TAOK1 expression in the SVZ area of brain slice was examined by immunohistochemical analysis, DAPI was used for nuclear staining. (**D**) TUNEL assay was performed to detect neuronal apoptosis of SVZ brain slice of sham and MCAO rats. (**E**) Expression of IL-1β, IL-6 and IL-8 in the blood samples collected from sham and MCAO animals were evaluated by ELISA (**$P<0.01$, ***$P<0.001$ *vs* Sham).

Overexpression of TAOK1 partially abolished the OGD-induced apoptosis

CCK-8 assay and EdU staining were performed to examine the effects of TAOK1 on cell proliferation, and flow cytometry analysis and TUNEL assay were performed to investigate the effects of TAOK1 on cell apoptosis and cell cycle. Compared with normal group, OGD-treated group showed a significant suppression of cell proliferation; compared with OGD+NC treated group, TAOK1 blocked cells under OGD (OGD+shRNA group) aggravated the OGD-induced proliferation suppression, whereas TAOK1 overexpressed cells under OGD (OGD+TAOK1 group) have partially reversed the OGD-induced proliferation suppression (***$P<0.001$ vs normal group, $^{###}P<0.001$ vs OGD+NC group, Figure 4A,B). In the cell cycle analysis, the cell number of OGD-treated group showed a significant up-regulation in G_0/G_1 phase and a down-regulation in S phase when compared with normal group (Figure 4C). The cell number of OGD+shRNA group showed a remarkable up-regulation in G_0/G_1 phase, and a down-regulation in S phase, whereas the OGD+TAOK1 group showed opposing trend with OGD+shRNA group when compared with OGD+NC group (Figure 4C). In the apoptotic analysis of flow cytometry and TUNEL assay, the cell apoptotic rate was significantly higher in OGD-treated group than normal group (Figure 4D,E). Compared with OGD+NC group, the cell apoptosis
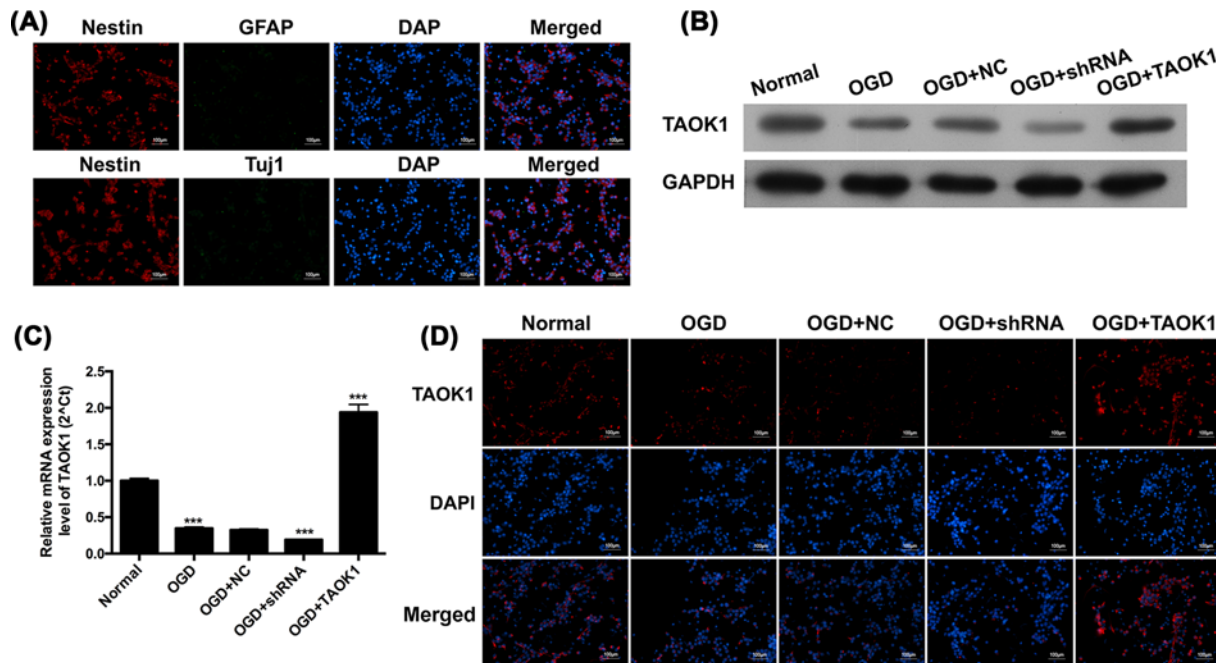
Figure 3. TAOK1 expression was significantly decreased post-OGD in neural stem cells
(**A**) Identification of neural stem cells by examining the corresponding types of molecular markers, Nestin, GFAP and Tuj1 with immunofluorescent (IF) staining. (**B,C**) Relative protein and mRNA expression of TAOK1 of TAOK1 blocked and overexpressed neural stem cells under OGD conditions were assessed by Western blotting and qRT-PCR, respectively (***$P<0.001$ vs Normal group). (**D**) Immunofluorescent staining was performed to examine the expression of TAOK1 in TAOK1 blocked and overexpressed neural cells under OGD conditions.

was markedly aggravated in OGD+shRNA group, whereas the cell apoptotic rate in OGD+TAOK1 group was significantly inhibited (Figure 4D,E). In addition, Western blotting was carried out to detect the protein expression of apoptotic-related proteins (Bcl-2, Bax, and cleaved-caspase-3) and cell cycle-related proteins (CyclinD1 and p21). The results showed that Bax, cleaved-caspase-3, and p-21 expressions were significantly up-regulated, whereas Bcl-2 and CyclinD1 expressions were significantly down-regulated in OGD group compared with normal group (Figure 5B). Compared with OGD+NC group, Bax, cleaved-caspase-3, and p-21 expressions in OGD+shRNA group were higher, whereas their expression in OGD+TAOK1 group were lower; Bcl-2 and CyclinD1 expressions in OGD+shRNA and OGD+TAOK1 groups exhibited opposing trends with Bax, Cleaved-caspase-3, and p-21 expression (Figure 5B).

Subsequently, to further investigate whether the ability of TAOK1 to partially offset the pro-apoptotic effect of OGD is dependent upon the intrinsic kinase activity of TAOK1. Kinase-inactive mutant plasmid (TAOK1^{K57A}) was constructed and transfected into OGD-induced cortical neural stem cells. The results from Western blotting analysis and immunofluorescent staining uncovered that the level of TAOK1 was notably aggrandized in OGD-treated cortical neural stem cells after transfection with TAOK1 or TAOK1^{K57A}, indicating the efficient transfections of TAOK1 and TAOK1^{K57A} (Supplementary Figure S2A,B). Simultaneously, we testified that the significant up-regulation of Bcl-2, down-regulation of Bax and cleaved-caspase-3, which were mediated by overexpression of TAOK1 in OGD-induced cortical neural stem cells, were significantly weakened after inactivation of the intrinsic kinase activity (Supplementary Figure S2A). Besides, we revealed that the reduction in apoptosis mediated by TAOK1 overexpression could be prevented by the inactivation of the intrinsic kinase activity (Supplementary Figure S2C,D). Therefore, we verified that the intrinsic kinase activity of TAOK1 determined the effect of TAOK1 on OGD-induced apoptosis.

Overexpression of TAOK1 partially reversed the OGD-induced up-regulation of IL-1β, IL-6, and IL-8

ELISA was then performed to detect the production of IL-1β, IL-6, and IL-8. Compared with normal group, OGD treatment significantly increased the production of IL-1β, IL-6, and IL-8 (**$P<0.01$, ***$P<0.001$ vs normal group, Figure 5A). Compared with OGD+NC group, IL-1β, IL-6, and IL-8 production were significantly increased in

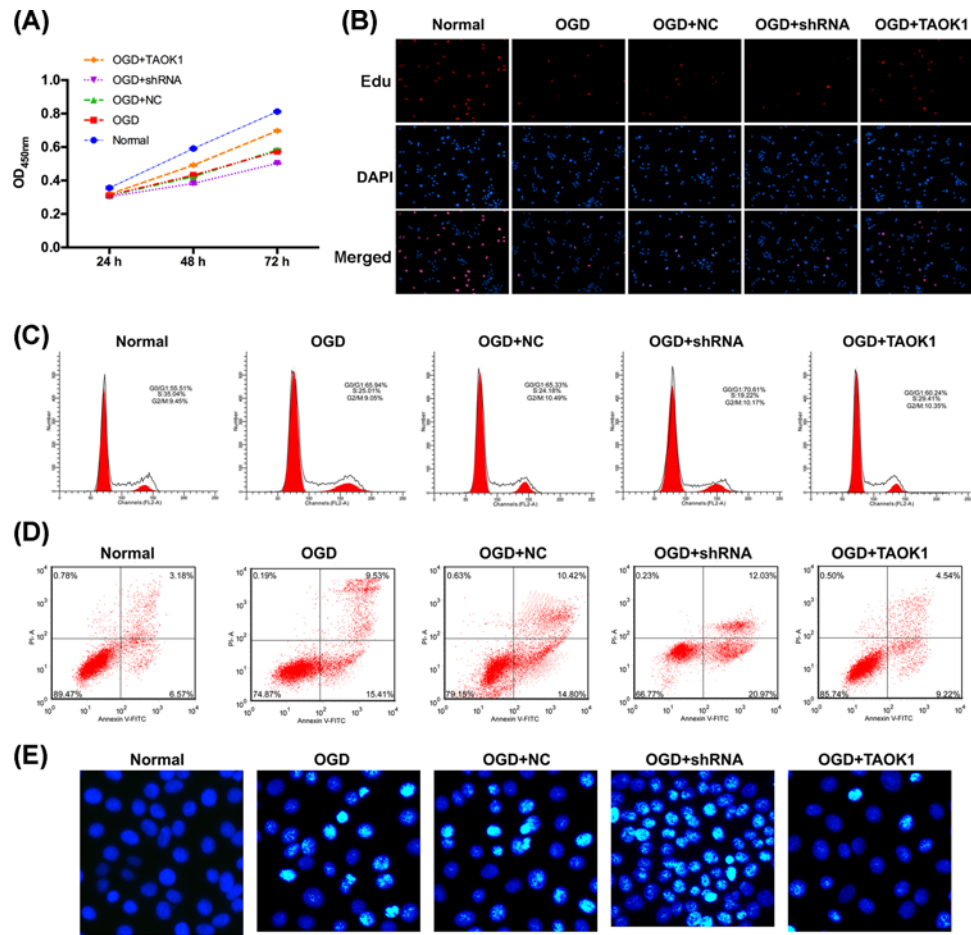**Figure 4. Overexpression of TAOK1 partially abolished the OGD-induced apoptosis**
(**A**,**B**) Cell proliferation of NC, TAOK1 and its shRNA treated neural cells under OGD conditions were evaluated by CCK-8 assay and Edu staining. (**C**) Cell cycle of NC, TAOK1 and its shRNA treated neural cells under OGD conditions were evaluated by flow cytometry. (**D**,**E**) Cell apoptosis of NC, TAOK1, and its shRNA treated neural cells under OGD conditions were assessed by flow cytometry and TUNEL assay.

OGD+shRNA group, whereas their productions were remarkably down-regulated in OGD+TAOK1 group (*$P<0.05$, **$P<0.01$ vs OGD+NC group, Figure 5A). In addition, the effects of TAOK1 on PI3K/AKT and MAPK signaling pathways were examined by detecting the expression of AKT/p-AKT, ERK/p-ERK, PI3K, and P38/p-P38 via Western blotting. The results showed that p-AKT and PI3K expressions were significantly reduced in OGD group compared with normal group. However, p-ERK and p-P38 expressions in OGD group showed opposing expression trends with p-AKT and PI3K (Figure 5B). Compared with OGD+NC group, p-AKT and PI3K expressions were lower in OGD+shRNA group, whereas higher in OGD+TAOK1 group. However, p-ERK and p-P38 expressions were higher in OGD+shRNA group, whereas lower in OGD+TAOK1 group (Figure 5B).

Discussion

In mammals, neural stem cells are mainly distributed in the ventromitic zone (VZ), subventricular zone (SVZ), corpus striatum, dentate gyrus, spinal cord etc [21]. SVZ is a major area for the generation of new neurons [22]. According to the literature, we found that a large number of studies have adopted the SVZ of MCAO model animals to explore the potential therapies for cerebral ischemic stroke. In our study, our results disclosed that TAOK1 was highly expressed in the SVZ of MCAO rats. In addition, we demonstrated that TAOK1 expression was significantly decreased in the MCAO rat model and OGD-induced cell model of ischemic stroke when compared with sham-operative rats and normal neutral stem cells, respectively. Moreover, the OGD-induced cell proliferation inhibition and apoptotic promotion could be partially abolished by TAOK1 overexpression in neural stem cells. However, the OGD-induced
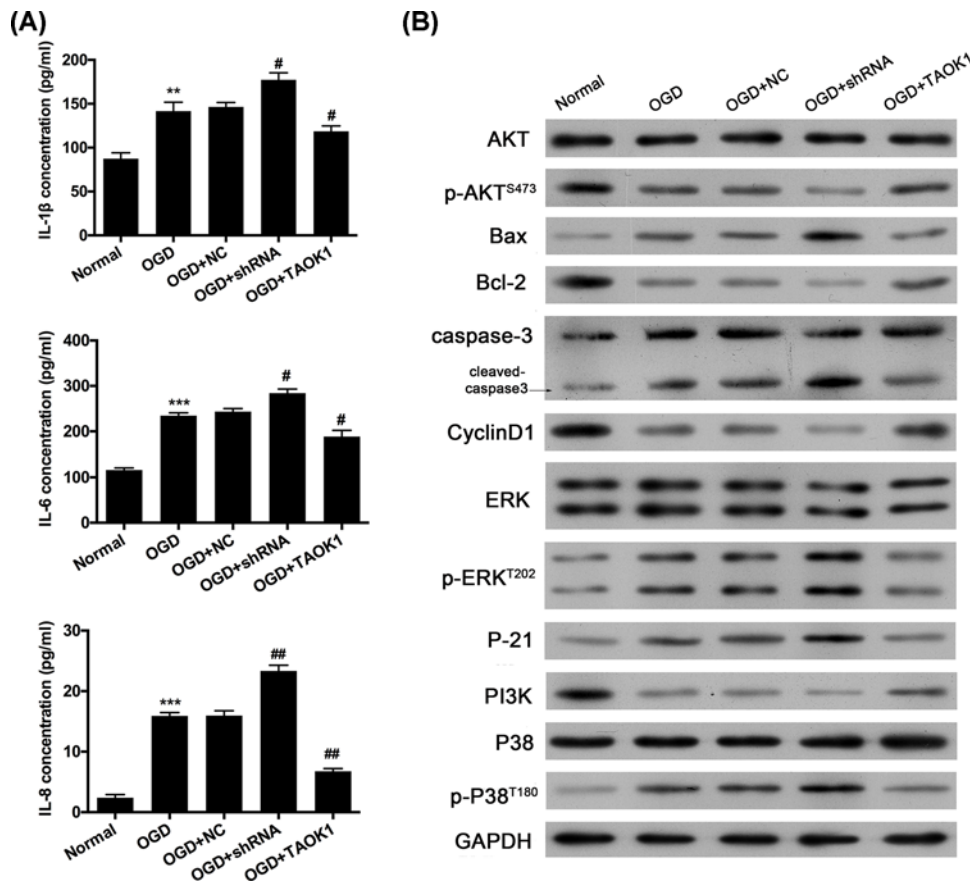
Figure 5. Overexpression of TAOK1 partially reversed the OGD-induced up-regulation of IL-1β, IL-6, and IL-8
(**A**) ELISA was carried out to examine the expression of IL-1β, IL-6, and IL-8 in NC, TAOK1 and shRNA treated neural cells under OGD conditions (**$P<0.01$, ***$P<0.001$ *vs* normal group; #$P<0.05$, ##$P<0.01$ *vs* OGD group). (**B**) Western blot assay was performed to analyze the protein expression of AKT/p-AKT, Bax, Bcl-2, Cleaved-caspase-3, CyclinD1, ERK/p-ERK, P-21, PI3K, and P38/p-P38 in normal, OGD, OGD+NC, OGD+shRNA, and OGD+TAOK1 groups.

cell injury was exacerbated by blocking TAOK1 expression. These findings suggested that TAOK1 is involved in the pathogenesis of ischemic stroke, and it might be a potentially effective therapeutic molecular target for ischemic stroke. Previous studies have mostly focused on the functions regarding the regulation of microtubule dynamics and mitotic progression [12]. To the best of our knowledge, this was the first time to reveal the involvement of TAOK1 in ischemic stroke.

Although the exact etiology of ischemic stroke remains largely unknown, increasing evidence has indicated that inflammation and its mediators play a critical role in ischemic stroke [23,24]. Under ischemic conditions, the production of inflammatory mediators in the ischemic brain tissues were significantly elevated from the resident microglia cells and infiltrating immune cells [25]. These inflammatory mediators act as a double-edged sword in ischemic stroke, as they not only exacerbate the brain tissue injury induced by ischemia in the acute stroke, but also contribute to the tissue recovery of the brain after stroke [23]. The present study showed that the production of IL-1β, IL-6, and IL-8 were markedly higher in the MCAO treated rats and OGD-induced neural stem cells than those in sham operative animals and normal cells. IL-1β was considered to be a critical contributor to ischemic induced brain injury, and evidence revealed that MCAO induced brain damage was significantly attenuated in IL-1β knockdown mice, whereas the damage caused by MCAO was exacerbated when IL-1β was directly administered into animals [26,27]. IL-6 is another pro-inflammatory cytokine that is involved in the pathogenesis of ischemic stroke [28]. Recent studies have demonstrated that IL-6 production was elevated during ischemic stroke conditions [28], which was consistent with our results. The increased inflammatory response caused by IL-6 might exacerbate the ischemic stroke induced brain injury, and the IL-6 overexpression was considered to be a biomarker of ischemic stroke outcome [29].

Moreover, in the present study, TAOK1 reversed the up-regulation of IL-1β, IL-6, and IL-8 induced by OGD *in vitro*. Previous studies suggested that TAOK1 could suppress the production of pro-inflammatory cytokines induced by IL-17, and it also inhibited the activation of p38, JNK, and ERK1/2 *in vitro* [30]. In the present study, we also found that TAOK1 could suppress the activation of p38 and ERK induced by OGD in neural stem cells.

Conclusion

TAOK1 expression was significantly down-regulated, however, IL-1β, IL-6 and IL-8 expression were up-regulated in MCAO rat model and OGD-induced neural stem cell model of ischemic stroke. In the *in vitro* cell model, TAOK1 reversed the OGD-induced cell injury, and up-regulated IL-1β, IL-6, and IL-8. In terms of the mechanism, the PI3K/AKT and MAPK signaling pathways were involved in the induction of TAOK1 effects in ischemic stroke. However, the present study is not perfect due to time and funding. For example, we only investigated the expression level of TAOK1 in SVZ of brains. In the future, we will further investigate the levels of TAOK1 in cortical and striatal regions, and explore the function and possible mechanism of TAOK1 on the neural stem cells in cortical and striatal regions.

Author Contribution

Y.W. conceived and designed the experiments. J.L., Z.L., L.W. and H.X. performed the experiments. J.L. and Z.L. analyzed the data. Y.W. and J.L. wrote the paper. All authors read and approved the final manuscript.

Competing Interests

The authors declare that there are no competing interests associated with the manuscript.

Abbreviations

CCK-8, cell counting kit-8; ECA, external carotid artery; ELISA, enzyme-linked immunosorbent assay; ERK, extracellular signal-regulated kinase; HIE, hypoxic–ischemic encephalopathy; IACUC, Institutional Animal Care and Use Committee; JNK, c-Jun N-terminal kinase; MAPK, mitogen-activated protein kinase; MCA, middle cerebral artery; MCAO, MCA occlusion; OGD, oxygen-glucose deprivation; PI, propidium iodide; qRT-PCR, quantitative real-time PCR; shRNA, short hairpin RNA; SVZ, subependymal ventricular zone; TAOK1, thousand and one kinase 1; TTC, 2,3,5-triphenyltetrazolium chloride.

References

1 du Plessis, A.J. (2009) Neurology of the newborn infant. Preface. *Clin. Perinatol.* **36**, xi–xiii, https://doi.org/10.1016/j.clp.2009.09.001

2 (2015) Global, regional, and national age-sex specific all-cause and cause-specific mortality for 240 causes of death, 1990-2013: a systematic analysis for the Global Burden of Disease Study 2013. *Lancet* **385**, 117–171, https://doi.org/10.1016/S0140-6736(14)61682-2

3 Fernandez-Lopez, D., Natarajan, N., Ashwal, S. and Vexler, Z.S. (2014) Mechanisms of perinatal arterial ischemic stroke. *J. Cereb. Blood Flow Metab.* **34**, 921–932, https://doi.org/10.1038/jcbfm.2014.41

4 Gooshe, M., Abdolghaffari, A.H., Aleyasin, A.R. et al. (2015) Hypoxia/ischemia a key player in early post stroke seizures: modulation by opioidergic and nitrergic systems. *Eur. J. Pharmacol.* **746**, 6–13, https://doi.org/10.1016/j.ejphar.2014.11.005

5 Sun, Y.Y., Lee, J., Huang, H. et al. (2017) Sickle mice are sensitive to hypoxia/ischemia-induced stroke but respond to tissue-type plasminogen activator treatment. *Stroke* **48**, 3347–3355, https://doi.org/10.1161/STROKEAHA.117.018334

6 He, L., He, R., Liang, R. et al. (2018) Protein expression profiling in the hippocampus after focal cerebral ischemia injury in rats. *J. Integr. Neurosci.* **17**, 149–158, https://doi.org/10.3233/JIN-170047

7 Ohshima, M., Taguchi, A., Sato, Y. et al. (2016) Evaluations of Intravenous administration of CD34+ human umbilical cord blood cells in a mouse model of neonatal hypoxic-ischemic encephalopathy. *Dev. Neurosci.* **38**, 331–341, https://doi.org/10.1159/000454830

8 Seet, R.C. and Rabinstein, A.A. (2012) Symptomatic intracranial hemorrhage following intravenous thrombolysis for acute ischemic stroke: a critical review of case definitions. *Cerebrovasc. Dis.* **34**, 106–114, https://doi.org/10.1159/000339675

9 Marder, V.J., Jahan, R., Gruber, T., Goyal, A. and Arora, V. (2010) Thrombolysis with plasmin: implications for stroke treatment. *Stroke* **41**, S45–S49, https://doi.org/10.1161/STROKEAHA.110.595157

10 Endo, A., Nagai, N., Urano, T. et al. (1998) Proteolysis of highly polysialylated NCAM by the tissue plasminogen activator-plasmin system in rats. *Neurosci. Lett.* **246**, 37–40, https://doi.org/10.1016/S0304-3940(98)00204-3

11 Moore, T.M., Garg, R., Johnson, C., Coptcoat, M.J., Ridley, A.J. and Morris, J.D. (2000) PSK, a novel STE20-like kinase derived from prostatic carcinoma that activates the c-Jun N-terminal kinase mitogen-activated protein kinase pathway and regulates actin cytoskeletal organization. *J. Biol. Chem.* **275**, 4311–4322, https://doi.org/10.1074/jbc.275.6.4311

12 Chen, Z., Hutchison, M. and Cobb, M.H. (1999) Isolation of the protein kinase TAO2 and identification of its mitogen-activated protein kinase/extracellular signal-regulated kinase kinase binding domain. *J. Biol. Chem.* **274**, 28803–28807, https://doi.org/10.1074/jbc.274.40.28803

13 Hutchison, M., Berman, K.S. and Cobb, M.H. (1998) Isolation of TAO1, a protein kinase that activates MEKs in stress-activated protein kinase cascades. *J. Biol. Chem.* **273**, 28625–28632, https://doi.org/10.1074/jbc.273.44.28625

14 Zihni, C., Mitsopoulos, C., Tavares, I.A., Ridley, A.J. and Morris, J.D. (2006) Prostate-derived sterile 20-like kinase 2 (PSK2) regulates apoptotic morphology via C-Jun N-terminal kinase and Rho kinase-1. *J. Biol. Chem.* **281**, 7317–7323, https://doi.org/10.1074/jbc.M513769200

15 Thies, E. and Mandelkow, E.M. (2007) Missorting of tau in neurons causes degeneration of synapses that can be rescued by the kinase MARK2/Par-1. *J. Neurosci.* **27**, 2896–2907, https://doi.org/10.1523/JNEUROSCI.4674-06.2007

16 Draviam, V.M., Stegmeier, F., Nalepa, G. et al. (2007) A functional genomic screen identifies a role for TAO1 kinase in spindle-checkpoint signalling. *Nat. Cell Biol.* **9**, 556–564, https://doi.org/10.1038/ncb1569

17 Zihni, C., Mitsopoulos, C., Tavares, I.A., Baum, B., Ridley, A.J. and Morris, J.D. (2007) Prostate-derived sterile 20-like kinase 1-alpha induces apoptosis. JNK- and caspase-dependent nuclear localization is a requirement for membrane blebbing. *J. Biol. Chem.* **282**, 6484–6493, https://doi.org/10.1074/jbc.M608336200

18 Yin, R., Guo, D., Zhang, S. and Zhang, X. (2016) miR-706 inhibits the oxidative stress-induced activation of PKCalpha/TAOK1 in liver fibrogenesis. *Sci. Rep.* **6**, 37509, https://doi.org/10.1038/srep37509

19 Patel, M., Cai, Q., Ding, D., Salvi, R., Hu, Z. and Hu, B.H. (2013) The miR-183/Taok1 target pair is implicated in cochlear responses to acoustic trauma. *PLoS ONE* **8**, e58471, https://doi.org/10.1371/journal.pone.0058471

20 Aleksandrova, M.A., Poltavtseva, R.A., Marei, M.V. and Sukhikh, G.T. (2016) Analysis of neural stem cells from human cortical brain structures *in vitro*. *Bull. Exp. Biol. Med.* **161**, 197–208, https://doi.org/10.1007/s10517-016-3375-5

21 Dori, I., Petrakis, S., Giannakopoulou, A. et al. (2017) Seven days post-injury fate and effects of genetically labelled adipose-derived mesenchymal cells on a rat traumatic brain injury experimental model. *Histol. Histopathol.* **32**, 1041–1055

22 Guan, J., Tong, W., Ding, W. et al. (2012) Neuronal regeneration and protection by collagen-binding BDNF in the rat middle cerebral artery occlusion model. *Biomaterials* **33**, 1386–1395, https://doi.org/10.1016/j.biomaterials.2011.10.073

23 Jin, R., Liu, L., Zhang, S., Nanda, A. and Li, G. (2013) Role of inflammation and its mediators in acute ischemic stroke. *J. Cardiovasc. Transl. Res.* **6**, 834–851, https://doi.org/10.1007/s12265-013-9508-6

24 Mao, L.-L., Hao, D.-L., Mao, X.-W. et al. (2015) Neuroprotective effects of bisperoxovanadium on cerebral ischemia by inflammation inhibition. *Neurosci. Lett.* **602**, 120–125, https://doi.org/10.1016/j.neulet.2015.06.040

25 Lambertsen, K.L., Biber, K. and Finsen, B. (2012) Inflammatory cytokines in experimental and human stroke. *J. Cereb. Blood Flow Metab.* **32**, 1677–1698, https://doi.org/10.1038/jcbfm.2012.88

26 Yamasaki, Y., Matsuura, N., Shozuhara, H., Onodera, H., Itoyama, Y. and Kogure, K. (1995) Interleukin-1 as a pathogenetic mediator of ischemic brain damage in rats. *Stroke* **26**, 676–680, https://doi.org/10.1161/01.STR.26.4.676

27 Boutin, H., LeFeuvre, R.A., Horai, R., Asano, M., Iwakura, Y. and Rothwell, N.J. (2001) Role of IL-1alpha and IL-1beta in ischemic brain damage. *J. Neurosci.* **21**, 5528–5534, https://doi.org/10.1523/JNEUROSCI.21-15-05528.2001

28 Herrmann, O., Tarabin, V., Suzuki, S. et al. (2003) Regulation of body temperature and neuroprotection by endogenous interleukin-6 in cerebral ischemia. *J. Cereb. Blood Flow Metab.* **23**, 406–415, https://doi.org/10.1097/01.WCB.0000055177.50448.FA

29 Waje-Andreassen, U., Krakenes, J., Ulvestad, E. et al. (2005) IL-6: an early marker for outcome in acute ischemic stroke. *Acta Neurol. Scand.* **111**, 360–365, https://doi.org/10.1111/j.1600-0404.2005.00416.x

30 Zhang, Z., Tang, Z., Ma, X. et al. (2018) TAOK1 negatively regulates IL-17-mediated signaling and inflammation. *Cell. Mol. Immunol* **15**, 794–802, https://doi.org/10.1038/cmi.2017.158